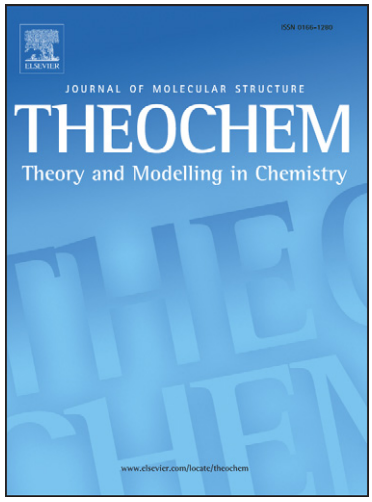

DFT Study of Electronic Properties, Structure and Spectra of Aryl Diazonium Cations

Boris F. Minaev, Sergey V. Bondarchuk, Mihai A. Gîrtu

PII: S0166-1280(09)00130-4
DOI: 10.1016/j.theochem.2009.02.022
Reference: THEOCH 11540

To appear in: *Journal of Molecular Structure: THEOCHEM*

Received Date: 30 November 2008
Revised Date: 16 February 2009
Accepted Date: 20 February 2009

Please cite this article as: B.F. Minaev, S.V. Bondarchuk, M.A. Gîrtu, DFT Study of Electronic Properties, Structure and Spectra of Aryl Diazonium Cations, *Journal of Molecular Structure: THEOCHEM* (2009), doi: 10.1016/j.theochem.2009.02.022

DFT Study of Electronic Properties, Structure and Spectra of Aryl Diazonium Cations

Boris F. Minaev,[a,*] Sergey V. Bondarchuk[a], Mihai A. Gîrțu[b,†]

[a]Department of Chemistry, B. Hmelnitskyi National University, Cherkassy, Ukraine
[b]Department of Physics, Ovidius University of Constanța, Constanța, Romania

Abstract

We report here Density Functional Theory calculations providing the electronic structure, IR absorption and Raman bands for a series of aryl diazonium cations, X-$C_6H_4N_2^+$, with different substituents (X = Cl, Br, F, NO_2, NH_2, CH_3, CF_3, CN, OH, OCH_3, COOH, $COOC_2H_5$, etc.) in the *ortho*-, *meta*- and *para*-positions. The DFT study allows the complete assignment of IR absorption bands, with good agreement with the experimental data, for the few cases where such data are available. For some IR bands we discuss the correlations between the vibrational frequencies and intensities and the nature and force of the mesomeric effect of the substituent. We also analyze the influence of the substituent, to better understand any changes in the activity of the cation as a reagent in the Meerwein reaction. The study of the N–N vibration frequency of the radical and the analysis of the orbital structure showed that the SOMO has a bonding character along the C–N link, hindering nitrogen elimination.

Key words: Aryl diazonium cations, vibrational frequency, density functional theory, Meerwein reaction

1. Introduction

Although historically, diazonium salts have been developed as important intermediates in the organic synthesis of dyes, aryl diazonium cations have continuously stirred interest as new applications have been found. Recently, the electrochemical reduction of an aryl diazonium salt has been established as a convenient procedure for the modification of carbon, silicon and metal surfaces [1-4]. It relies on the electrochemical generation of aryl radicals, which then react with a surface, such as a carbon substrate, to form a covalent bond between a carbon atom of the surface and the aryl group. The resulting surfaces can be used as modified electrodes for biosensor applications, as templates for metal particle formation, to enhance adhesion between carbon fibers and a resin and corrosion protection [5,6].

Aromatic diazonium salts are also widely used in organic chemistry as reactants in different syntheses. For instance, the process of nitrogen elimination from diazonium cations is a fundamental stage of the Meerwein [7] and Sandmeyer [8,9] reactions. For both these reactions, the improvement of the yield depends on the usage of diazonium salts, which lose nitrogen effectively. A measure of diazonium cations stability with respect to the C–N bond cleavage (and at the same time an indicator of their activity as electrophilic agents) can be the frequencies of the stretching vibrations of the C–N≡N group [10]. The determination of the corresponding vibrational modes is, therefore, of high importance, however, the low thermal stability of diazonium compounds often prevents extensive IR and Raman spectroscopy experimental studies. For instance, available in the literature are the vibrational frequencies of the N≡N mode only.

Different modifications of Meerwein arylation may involve the usage of reagents generating diazonium cations. As arylative agents 3,3-dymethyl-1-threeazenes [11], aryl diazonium tetrachlorocuprates(II) [12] or aryl diazonium tetrachlorozincates(II) [13] have been efficiently

* bfmin@rambler.ru
† girtu@univ-ovidius.ro

used. Double diazonium salts with complex anions like $AlCl_4^-$ [14], $TlCl_3^{2-}$ [15], $SbCl_3$ and $HgCl_2$ [16] have been synthesized and their structures have been resolved. To determine the composition of such salts a melting point measurement or an elementary analysis are usually used. However, the melting point measurement cannot always give a reliable description of diazonium salts because of their thermal decomposition. Similarly, the elemental analysis does not always succeed to give a precise enough description of the composition for each individual salt. Therefore, a more accurate method of determination of the structure of diazonium salts is based on the IR-spectroscopy. Consequently, accurate IR absorption and Raman band calculations are also needed.

It has been argued [10,17,18] that the Hartree-Fock method severely overestimates (by 200-500 cm^{-1}) the high frequencies (greater than 1600 cm^{-1}), considerably underestimates the low ones ($\leq$ 300 cm^{-1}) and systematically overestimates (by 100-200 cm^{-1}) the rest ones because of not taking into account electron correlations. Taking into account such electron correlations by means of MP2 theory, does not improve considerably the results. In contrast, the DFT /B3LYP method is relatively more successful: at high frequencies ($\geq$ 1600 cm^{-1}) the overestimation is lower, 100-150 cm^{-1}, at low frequencies ($\leq$ 300 cm^{-1}) the underestimation is even smaller, and at moderate frequencies the overestimation is of about 20-50 cm^{-1} [10,19]. Earlier calculations of diazonium salts were carried out by the PNDO [20], SCF PPP [21] and CNDO/2 [22] methods, using a fixed geometry. These calculations, which were performed in the π-approximation, without account of electron correlation, provided only a qualitative description of the charge distribution.

In this paper, we interpret and generalize the results of previous investigations on the basis of density functional theory (DFT). We also report new results for the molecular structure as well as the IR and Raman spectra of the some aryl diazonium cations, $X\text{-}C_6H_4N_2^+$, with different substituents (X = Cl, Br, F, NO_2, NH_2, CH_3, CF_3, CN, OH, OCH_3, COOH, $COOC_2H_5$, etc.) in the *ortho*-, *meta*- and *para*-positions.

2. Methods of calculations

The geometry optimization was performed starting with the molecular mechanics method AMBER [23]. The resulting geometry was further refined by semi-empirical self-consisted field (SCF) Hartree-Fock method at the PM3 level of approximation [24]. Based on these results the stationary geometries and vibrational spectra of phenyl diazonium substituted cations were subsequently performed using the DFT method [25] at B3LYP [26,27]/6-31G** level [28]. This method allows an addition of polarization functions for a better account of atomic polarization. We performed geometry optimization at the restricted DFT (B3LYP) level for the diazonium cations [29]. The calculation of the phenyl diazonium radical, which is formed during diazoreduction was carried out using the unrestricted DFT (B3LYP) level. Vibrational frequencies and intensities of the IR absorption bands are calculated for all optimized structures.

We also compared our previous PM3 results [30] with the DFT values in the present paper for the frequencies, forms, and intensities of vibrations in the IR-spectra of different phenyl diazonium substituted cations. All DFT calculations were performed using the Gaussian03 program suite [31]. Some of the present calculations were carried out at the Stockholm Centre of Physics, Astronomy and Biotechnology (SCFAB).

3. Results and Discussion

3.1 Optimized geometry

The atom labeling for the phenyl diazonium cation is shown in Fig. 1.

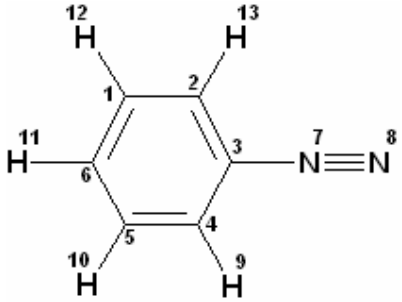

Fig. 1. Atom labeling for the phenyl diazonium cation

With just one exception, *o*-nitrophenyl diazonium, all cations studied display a planar structure. Both of the nitrogen atoms lie in the ring plane, the $\angle_{C(3)-N(7)-N(8)}$ angle being about 180º for all cations except for *o*-nitrophenyl diazonium, for which the angle is 169.7º. The deviation in this particular case may appear due to an electrostatic attraction of the N(7) nitrogen atom to the nearby oxygen atom of the nitro group lying in plane of the cation.

The calculated C(3)–N(7) bond lengths and the N(7)–N(8) bond lengths are collected in Table 1.

Table 1. The N(7)–N(8) and the C(3)–C(7) bond lengths of aryl diazonium cations X-$C_6H_4N_2^+$ calculated by DFT/B3LYP/6-31G**.

X-	Bond length, Å	
	N(7)–N(8)	C(3)–N(7)
H	1.116	1.375
o-**Cl**	1.116	1.369
m-**Cl**	1.115	1.377
p-**Cl**	1.117	1.368
o-**NO_2**	1.114	1.386
m-**NO_2**	1.114	1.380
p-**NO_2**	1.114	1.381
o-**CH_3**	1.117	1.371
m-**CH_3**	1.116	1.374
p-**CH_3**	1.117	1.368
o-**OH**	1.121	1.355
m-**OH**	1.116	1.375
p-**OH**	1.120	1.359
o-**OCH_3**	1.118	1.358
m-**OCH_3**	1.115	1.377
p-**OCH_3**	1.121	1.357
o-**$COOC_2H_5$**	1.118	1.361
p-**$COOC_2H_5$**	1.119	1.361
p-**F**	1.117	1.368
p-**Br**	1.118	1.367
p-**NH_2**	1.124	1.350
p-**COOH**	1.115	1.377
p-**SO_3H**	1.115	1.378
p-**C≡N**	1.116	1.376
2,4,6-**NO_2**	1.110	1.397
2,4,6-**OH**	1.121	1.342
p-**CF_3**	1.115	1.378
p-**$N^+(CH_3)_3$**	1.112	1.393

As it can be seen from Table 1 the longest C(3)–N(7) bond observed is in the case of X = 2,4,6-NO_2 (1.397 Å), and the shortest one for X = 2,4,6-OH (1.342 Å). Meanwhile, the N(7)–N(8) bond length varies from 1.110 Å (2,4,6-NO_2) to 1.124 Å (*p*-NH_2). A reason for such deviations in the indicated

bond lengths is the nature of the mesomeric effect of the substituent in the benzene ring, influencing the structure of the corresponding cation, effect discussed in more detail in the following section.

According to the experimental data based on X-ray analysis of benzene diazonium chloride [32], the C(3)–N(7) bond length is 1.385 Å; the N(7)–N(8) bond length is 1.097 Å, and the C(3)–N(7)–N(8) atoms are colinear. Similar results were obtained later for benzene diazonium tetrafluoroborate ($r_{C(3)–N(7)}$ = 1.415 Å, $r_{N(7)–N(8)}$ = 1.083 Å, $\angle_{C(3)–N(7)–N(8)}$ = 179.5°) [33]. Based on the relatively good agreement between the calculations and the experiment we conclude that the DFT/B3LYP method is reliable even with the 6-31G** basis set. The same trends have been obtained before in PM3 approximation [30].

The analysis of atomic charges on the diazonium group shows a $N(7)^{+}{\equiv}N(8)^{-}$ polarization, with a high negative charge density on N(8) for most systems. In the cases of strong electron acceptors located in the *ortho*- position with respect to the diazonium group or for substituents such as *p*-$N^{+}(CH_3)_3$ there is a positive charge on the edge nitrogen atom. The total charge on the diazonium group is about +0.1 for all phenyl diazonium substituted cations considered.

The vibration spectrum of phenyl diazonium cation consists of 33 normal modes. Calculated frequencies, intensities and form of vibration bands are given in Table 2. The vibration mode labeling is presented in the order of increasing vibration frequencies and the description of the vibration forms was performed in the standard letter notation.

The response of the electron system to nuclear vibrations varies for different types of vibrations. Most of all, the vibration intensity changes are significant, as they correlate with the speed of the dipole moment changes during nuclei motion away from the equilibrium point.

Table 2. Frequencies, intensities and depolarization ratio (p) of normal modes in IR and Raman spectra of phenyl diazonium cation calculated by DFT B3LYP 6-31 G** method.

Mode	v, cm^{-1}	*I*, km/mol	Raman, A^4/AMU	Depolarization ratio, (p)	Vibrational mode*
1	147	0.087	0.625	0.750	$\rho[\tau$ Ar, N(7)–N(8)]
2	180	0.565	3.728	0.750	$\delta[b$ C(3)–N(7)–N(8)]
3	391	0.374	2.108	0.750	$\rho[\tau$ Ar]; boat transform
4	393	0.265	0.002	0.750	$\rho[\tau$ Ar]; twist transform
5	463	1.081	9.882	0.374	$\delta[b$ C(1)–C(6)–C(5), C(2)–C(3)–C(4)]
6	550	1.428	1.767	0.750	$\delta[b$ Ar]
7	557	1.144	1.773	0.750	$\rho[\tau$ Ar]; boat transform; $\delta[b$ C(3)–N(7)–N(8)
8	627	1.632	5.062	0.750	ν_{as}[C–C]Ar; $\delta[b$ C(3)–N(7)–N(8)]
9	661	19.448	0.001	0.750	$\rho[\tau$ Ar]; arm-chair transform
10	771	57.222	0.377	0.750	$\rho[\omega$ C–H]; out of plane C(3)
11	772	0.025	9.501	0.103	$\delta[b$ C(5)–C(6)–C(1)]
12	836	0.000	3.297	0.750	$\rho_{as}[\tau$ Ar]; $\rho[\omega$ C–H]
13	965	1.487	1.368	0.750	$\rho_{as}[\tau$ Ar]; $\rho[\omega$ C–H]
14	998	0.000	0.347	0.750	$\rho[\tau$ Ar]; twist transform
15	1011	4.590	22.99	0.102	$\delta[b$ Ar]
16	1040	0.179	0.42	0.750	ν_{sym}[C(1)–C(6), C(6)–C(5)]
17	1041	0.231	18.72	0.142	$\rho[\tau$ Ar]; arm-chair transform
18	1125	4.073	1.77	0.750	$\delta[b$ C–CH]Ar
19	1143	136.739	5.163	0.750	ν[C–N]
20	1211	1.220	4.292	0.585	$\delta[b$ C–H]Ar
21	1221	0.634	0.687	0.750	ν_{sym}[C(1)–C(2), C(4)–C(5)]; $\delta[b$ C–H]
22	1360	0.261	36.92	0.176	$\delta(b$ C–CH]Ar;
23	1386	22.228	0.681	0.750	ν_{as}[C–C] Ar; "Keküle" vibration
24	1501	24.542	1.975	0.750	$\delta[b$ C–CH]Ar;
25	1503	1.075	0.492	0.472	$\delta[b$ C–CH]Ar;
26	1614	0.504	92.17	0.596	ν_{as}[C–CH]Ar;
27	1622	114.307	0.242	0.750	ν_{sym}[C–C]Ar; "Quinoid" vibration
28	2349	278.716	410.86	0.328	ν[N–N]
29	3224	0.254	49.90	0.579	ν_{sym}[C–H] ring
30	3233	0.387	98.87	0.750	ν_{as}[C–H] ring
31	3235	4.651	41.80	0.682	ν_{sym}[C–H] ring
32	3243	10.605	7.092	0.750	ν_{as}[C–H] ring
33	3245	0.032	287.79	0.111	ν_{sym}[C–H] "breathing"

***Abbreviations:** ν-stretch; ρ-out-of-plane deformation (τ-rotation, ω-umbrella); δ-in-plane deformation (*r*-rocking, *b*-scissor).

3.1 The N–N Vibration Band

The experimental N–N vibration frequencies (in dimethylformamide (DMFA), as solvent) [34] and the calculated ones are presented in Table 3. It can be seen that the overestimation of the

frequencies calculated with the DFT method does not exceed 66 cm^{-1}, far less than the 270 cm^{-1} overestimation obtained when using the PM3 method [30].

Table 3. Comparison of experimental (in DMFA [34]) and calculated (DFT/B3LYP/6-31G**) vibration frequencies of the N≡N absorption bands for X-$C_6H_4N_2^+$ cations.

X-	$\nu N{\equiv}N_{Exper}$	$\nu N{\equiv}N_{Calc}$	ν_E/ν_C
o-**OH**	2256	2303	0.9796
m-**OH**	2292	2344	0.9778
p-**OH**	2253	2318	0.9720
o-**CH_3O**	2274	2330	0.9760
m-**CH_3O**	2295	2352	0.9758
p-**CH_3O**	2255	2312	0.9753
o-**CH_3**	2275	2337	0.9735
m-**CH_3**	2293	2345	0.9778
p-**CH_3**	2276	2335	0.9747
H	2298	2348	0.9787
o-**Cl**	2293	2345	0.9778
m-**Cl**	2308	2352	0.9813
p-**Cl**	2298	2334	0.9846
p-**Br**	2298	2331	0.9858
o-**$COOC_2H_5$**	2301	2356	0.9767
p-**$COOC_2H_5$**	2309	2346	0.9842
o-**NO_2**	2299	2365	0.9721
m-**NO_2**	2315	2359	0.9813
p-**NO_2**	2314	2361	0.9801

The presence of substituents into the aromatic ring leads to wide shifts of the N–N absorption band. The ratio between the experimental and calculated frequencies varies only between 0.9720 and 0.9858, with most values around the average ratio of 0.9782. Using as scaling factor the average ratio of 0.9782 we obtain for the mid-infrared region quantitative coincidence of the N–N frequencies for almost all X-$C_6H_4N_2^+$ cations, including X=H. Similar scaling factors are typically involved in the comparison of the experimental and theoretical vibrational frequencies [35,36]. We note that we observed a similar good agreement between the frequencies and intensities of IR bands derived from DFT and PM3 calculations for both mid- and far-infrared region (ν<1500 cm^{-1}).

The high sensitivity of the diazonium group to the nature of the substituent is reflected by the shift of the vibration frequency, which can be correlated with the force of the mesomeric effect of the substituent. As our calculations show, electron withdrawing groups have the tendency to increase the frequency and the N–N bond order and to decrease the absorption intensity, in good agreement with experiments [34]. The electron donor substituents cause the inverse effect. The mesomeric influence of the substituent on the C(3)–N(7) and the N(7)–N(8) bond lengths as well as on the bond orders of the diazonium cation is illustrated in Scheme 1.

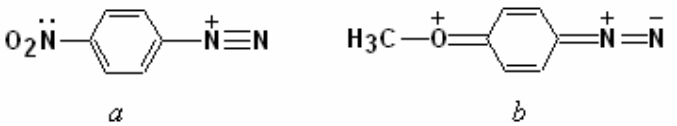

a *b*

Scheme 1. Illustration of the mesomeric influence of the substituent on two X-$C_6H_4N_2^+$ cations: a) X = *p*-NO_2 and b) *p*-OCH_3.

As it can be seen from Table 4, the values of the N–N frequency and vibration intensity are 2361, 2349, and 2312 cm^{-1} and 262.7, 278.7, and 593.4 km mol^{-1} for X = *p*-NO_2, H, and *p*-OCH_3, respectively. The decrease in N–N bond order when moving from X = *p*-NO_2 to X = *p*-OCH_3 is correlated with a strong increase in absorption intensity. We must stress, however, that such

correlations are observed only for *para*-substituted diazonium cations. The N–N vibration frequency and intensity is presented in Table 4 for various other substituents.

Groups with very strong +*M*-effect (i.e. NH_2, OCH_3) lead to huge IR intensities 702.8 and 593.4 km·mol^{-1} respectively, while effective π-electron acceptors in aromatic ring such as *p*-$N^+(CH_3)_3$, *o*-NO_2, *p*-NO_2 cause dramatic decreases of the vibration intensities 124.2, 141.9 and 262.7 km·mol^{-1}, respectively. An even more noticeable decrease of the vibration intensity takes place in 2,4,6-trinitrophenyl diazonium, where it is only 46.1 km·mol^{-1}. We also note that the expected increase in intensity for 2,4,6-trihydroxyphenyl diazonium is not observed. The value obtained, 401.7 km·mol^{-1}, is likely due to the rising influence of the –*I*-effect of the three hydroxy groups.

The plots of the N–N vibration frequency and intensity against Hammett constants show, to a good approximation, linear behavior (see Fig. 2).

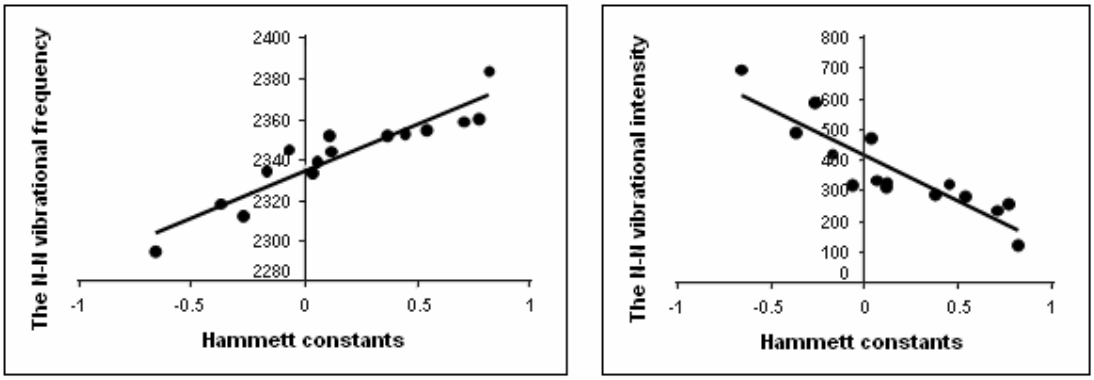

Fig. 2. Correlation of the N–N vibrational frequencies (left) and intensities (right) with the Hammett constants.

Summarizing this section, the process of nitrogen loss is facilitated if the amount of cation having the resonance structure *a* in Scheme 1 is increased. Our results justify the higher yields of Meerwein arylation products when such diazonium salts are used.

3.2 The C–N–N Fragment Vibrations

The absorption band at 2160-2300 cm^{-1} was assigned [37] as a vibration of the fragment C–N–N. We question this assignment as the analysis of the IR spectra of diazonium cations indicates that this band is the N–N stretch only, with no contribution from the aromatic ring. A more detailed analysis of IR spectra allows us to identify several other vibrations, which are more likely related to the C–N–N fragment. Among them we observed in-plane "rocking" and out-of-plane "umbrella" C–N–N deformations, which affect the benzene ring. Figure 3 shows the atom displacement vectors in Ph–N_2^+.

Table 4. Several vibrational bands of aryl diazonium cations X-$C_6H_4N_2^+$ calculated by DFT/B3LYP/6-31G**.

X-	*v*[N–N]		*v*[C–N]		"Keküle" vibration		"Quinoid" vibration		v_{as}[C–CH]Ar	
	v, cm^{-1}	*I*, $km \cdot mol^{-1}$	*v*, cm^{-1}	*I*, $km \cdot mol^{-1}$	*v*, cm^{-1}	*I*, $km \cdot mol^{-1}$	*v*, cm^{-1}	*I*, $km \cdot mol^{-1}$	*v*, cm^{-1}	*I*, $km \cdot mol^{-1}$
H	2349	278.7	1143	136.7	1386	22.2	1622	114.3	1614	0.5
***o*-Cl**	2345	240.8	1162	67.4	1370	38.6	1618	127.4	1597	24.3
***m*-Cl**	2352	287.4	1160	187.3	1380	24.9	1611	37.4	1595	61.4
***p*-Cl**	2334	472.9	1162	127.5	1366	7.1	1619	396.1	1577	2.2
***o*-NO_2**	2365	141.9	1171	94.8	1396	6.4	1628	93.2	1607	64.4
***m*-NO_2**	2359	240.1	1164	75.7	1384	83.2	1622	39.5	1612	7.5
***p*-NO_2**	2361	262.7	1134	118.9	1384	48.1	1624	111.2	1613	36.0
***o*-CH_3**	2337	279.6	1117	51.8	1369	35.0	1635	92.5	1601	28.7
***m*-CH_3**	2345	319.9	1143	68.0	1387	28.3	1604	74.2	1632	29.5
***p*-CH_3**	2335	420.6	1157	194.5	1372	11.1	1630	290.7	1586	0.1
***o*-OH**	2303	349.4	1126	29.1	1416	1.3	1656	155.4	1591	64.3
***m*-OH**	2344	332.0	1134	88.2	1409	76.3	1602	39.0	1646	103.8
***p*-OH**	2318	491.5	1176	315.8	1410	75.4	1653	474.9	1593	49.1
***o*-OCH_3**	2330	333.7	1053	6.2	1384	4.8	1646	189.2	1597	77.2
***m*-OCH_3**	2352	315.9	1120	42.3	1394	31.0	1594	93.1	1636	127.2
***p*-OCH_3**	2312	593.4	1173	300.7	1383	199.5	1647	586.4	1571	35.3
***o*-$COOC_2H_5$**	2335	303.3	1135	37.4	1373	36.1	1630	161.9	1597	58.1
***p*-$COOC_2H_5$**	2322	566.5	1168	149.2	1374	44.2	1633	496.3	1571	24.1
***p*-F**	2339	338.4	1159	192.5	1378	7.7	1642	390.0	1598	9.8
***p*-Br**	2331	565.2	1162	189.1	1365	6.4	1615	435.6	1573	1.8
***p*-NH_2**	2295	701.9	1188	237.7	1396	0.0	1658	293.3	1567	3.9
***p*-COOH**	2353	322.5	1140	166.0	1374	21.3	1631	94.0	1593	4.1
***p*-SO_3H**	2356	330.0	1138	85.0	1368	76.9	1619	144.5	1597	0.4
***p*-C≡N**	2342	460.2	1144	199.9	1363	15.4	1635	249.3	1579	1.1
2,4,6-NO_2	2398	46.1	1130	86.3	1387	7.0	1622	160.6	1615	26.5
2,4,6-OH	2318	401.7	1254	21.7	1426	151.8	1680	759.7	1615	227.4
***p*-CF_3**	2355	283.0	1139	131.7	1378	5.0	1642	68.5	1601	0.5
***p*-$N^+(CH_3)_3$**	2384	124.2	1133	16.0	1360	29.7	1627	147.6	1614	3.1

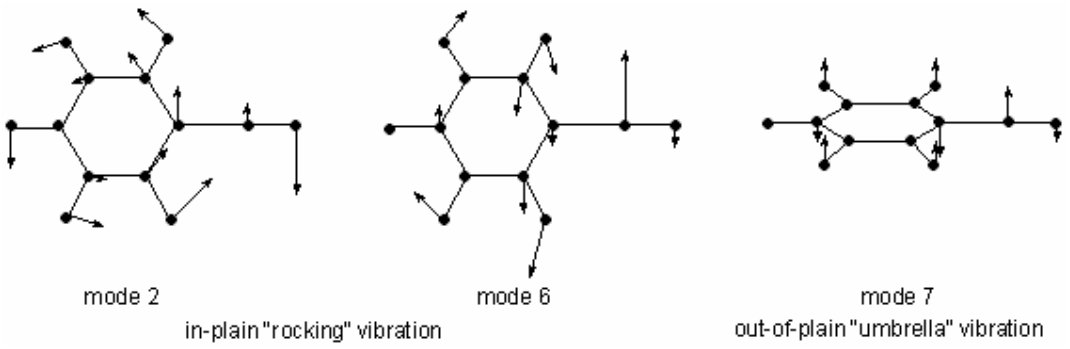

Fig. 3. Deformational vibrations of the C–N–N fragment for the phenyl diazonium cation.

These vibrations lie in the far-infrared region mostly and have very small intensities. By contrast, the C–N stretch is one of the most intense vibration bands for a great number of phenyl diazonium substituted cations, justifying some special attention in the following section.

C–N Stretch

One of the most characteristic vibrations for aryl diazonium cations is the C–N stretch (Table 4). This vibration lies in the mid-infrared region and varying in range of 1125-1170 cm^{-1} for most of phenyl diazonium substituted cations. A defining feature of this vibration is the in-plane ring deformation that causes the C–N stretch, leading to a motion of the hydrogen atoms in *ortho-* and *meta*-positions. The presence of a substituent in the *ortho*-position, which is the most involved in the vibration, causes a decrease of the IR intensity. In contrast, m*eta-* and especially *para-*substituted aryl diazonium cations have higher intensities for the same absorption band. A linear dependence of the C–N vibration frequencies on Hammett constants is presented below.

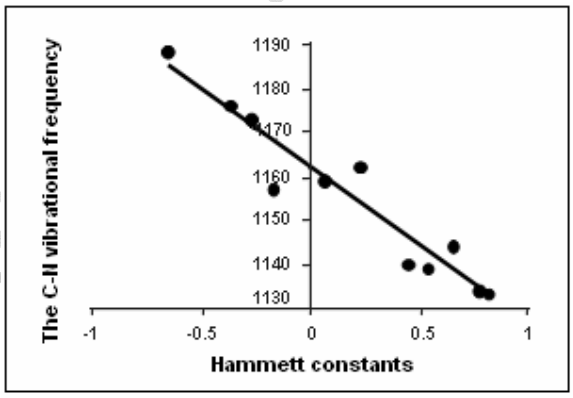

Fig. 4. Influence of Hammett constants on the C–N vibrational frequencies.

The electron acceptor substituents tend to form the structure *a* in Scheme 1, decreasing the vibration frequency, whereas π-electron donors cause the increase of the C–N bond order and of the frequency (see Table 4).

3.3 "Keküle" Vibration

Another interesting vibration, which is absolutely aromatic, is the "Keküle" vibration (an oscillation of double bonds). According to the experimental data [38] this vibration frequency is 1310 cm^{-1} for unsubstituted benzene. Surprisingly, the "Keküle" vibration frequency calculated by means of the PM3 method (1302 cm^{-1}) was closer to the experimental value than that obatined using the DFT

method (1354 cm^{-1}). Extending the comparison of the "Keküle" vibration frequencies calculated with PM3 [30] and DFT (Table 4) overall aryl diazonium cations studied, we note a systematic trend. Based on our results, we observe that the ratio between the frequencies obtained by PM3 and DFT for a number of diazonium cations is 1.009. We therefore propose the use of more accessible semi-empirical calculations, together with scaling factors (such as the ratio menioned above) for predicting frequencies, intensities, and forms of vibrations in mid-infrared region.

3.4 "Quinoid" Vibration

This vibration band is one of the most intense ones for all the aryl diazonium cations considered in this paper. The "quinoid" vibration (QV) is the C(1)–C(2) and the C(4)–C(5) stretch and varies in the range of 1594-1680 cm^{-1}. The frequencies of QV are strongly depended on the structure of the ion. The quasi-quinoid structure (Scheme 1, *b*) with higher C(1)–C(2) and C(4)–C(5) bond orders cuases the increase of the vibration frequencies, as shown in Fig. 5.

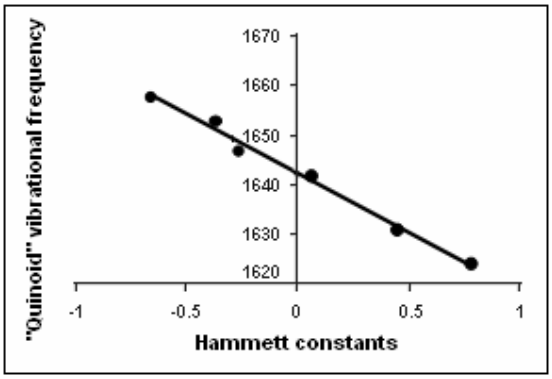

Fig. 5. "Quinoid" vibration frequencies as functions of Hammett constants.

The careful analysis of the aryldiazonia infrared spectra indicates that there is one more vibration lying close to the "quinoid" vibration, but with much smaller intensities compared to the ones of QV. This vibration mode can be assigned to the C(2)–C(3) and the C(5)–C(6) stretch. We label it ν_{as}[C–CH]Ar and note that it is very similar with the QV.

Diazonium cations with substituents in the *ortho*- and *meta*-positions have very distorted forms of the QV and ν_{as}[C–CH]Ar vibrations. Thus, it is difficult to assign them on the basis of pure visualization. The ν_{as}[C–CH]Ar vibration has lower frequencies compared to QV, the difference being of about 30 cm^{-1}. These two vibrations create characteristic doublets on the IR spectra plots. In the case of *para*-substituted arildiazonia, QV intensities are significantly higher than those for the ν_{as}[C–CH]Ar vibration. In contrast, for the *ortho*- and *meta*-substituted cations the values of the intensity become comparable. Moreover, in the case of the *m*-CH_3, *m*-OH and *m*-OCH_3 substituted cations a transposition of vibrational bands also takes place.

Some parameters of the electronic structure of substituted aryl diazonium cations are collected in Table 5.

Table 5. Electronic structure parameters (orbital energies, absolute enthalpies and dipole moment) of aryl diazonium cations X-$C_6H_4N_2^+$ calculated by DFT/B3LYP/6-31G**.

X–	$-E_{HOMO}$, eV	$-E_{LUMO}$, eV	$-H^0$, a. u.	μ, D
H	12.4740	8.0570	340.8472	0.5
***o*-Cl**	12.0707	8.1283	800.4337	3.3
***m*-Cl**	11.8157	8.2244	800.4328	5.1
***p*-Cl**	12.0435	8.0527	800.4376	4.8
***o*-NO_2**	12.9450	8.5770	545.3234	6.7
***m*-NO_2**	12.2427	8.5626	545.3248	8.8
***p*-NO_2**	12.1736	8.7131	545.3235	9.6
***o*-CH_3**	12.0250	7.8382	380.1716	0.6
***m*-CH_3**	11.9532	7.8763	380.1701	1.4
***p*-CH_3**	12.1464	7.7525	380.1832	1.2
***o*-OH**	11.7017	7.9095	416.0605	1.6
***m*-OH**	11.4119	7.9904	416.0634	2.6
***p*-OH**	11.7107	7.5525	416.0748	1.6
***o*-OCH_3**	11.3243	7.4883	455.3932	0.8
***m*-OCH_3**	10.9733	7.8140	455.3852	2.3
***p*-OCH_3**	11.3352	7.3403	455.3965	1.7
o-$COOC_2H_5$	11.5229	7.6037	608.0561	5.3
p-$COOC_2H_5$	11.5722	7.4981	608.0605	6.6
***p*-F**	12.5273	8.0423	440.0771	3.4
***p*-Br**	11.6274	7.9819	2911.9477	7.3
***p*-NH_2**	10.8549	6.9936	396.2416	2.4
***p*-COOH**	11.5953	8.4391	529.4033	9.2
***p*-SO_3H**	12.1322	8.4361	964.6177	10.7
***p*-C≡N**	12.5213	8.5449	433.0704	7.1
2,4,6-NO_2	12.7812	9.5468	954.2675	3.4
2,4,6-OH	11.1616	2.3307	566.5396	2.4
***p*-CF_3**	12.7719	8.3591	677.8773	9.4
***p*-$N^+(CH_3)_3$**	16.1241	11.4095	514.3833	0.1

3.5 Diazenyl Radical Calculations

For diazonium cations both the chemical and the electrochemical reduction are characteristic, leading to a diazenyl radical formation. Thermodynamically, the reduction propensity is determined by the LUMO energy [39]. The nitrogen elimination during the Meerwein reaction is considered as a process initiated by the reduction of diazonium cation into the radical.

The previous calculations of diazenyl radicals, performed using the PNDO method [20], claimed that the energy difference resulting from the fragmentation of $C_6H_5N_2^{\bullet}$ with simultaneous nitrogen loss (see Scheme 2) is about 950 kJ. Using more accurate methods, such as DFT, this difference was found to be not higher than 112.09 kJ, suggesting that the gain in energy is not as high. Obviously, nitrogen loss can occur through different intermediate species.

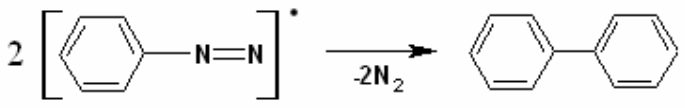

Scheme 2. Fragmentation of diazenyl radical with biphenyl formation

In contrast, our calculations show that the lowest unoccupied molecular orbital (LUMO) in diazonium cations is a bonding orbital along the C–N link (see Fig. 6). Thus, addition of one more electron on this molecular orbital during the radical formation will strengthen the C–N bond and hinder the elimination of the N_2 molecule.

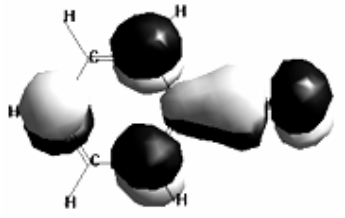

Fig. 6. The lowest unoccupied molecular orbital in phenyl diazonium cation.

The calculation of the diazenyl radical shows that the linear C(3)–N(7)–N(8) arrangement distorts, the $\angle_{C(3)–N(7)–N(8)}$ bond angle being equal to 125.3°. Moreover, the C(3)–N(7) and the N(7)–N(8) bonds lengthen to 1.457 Å and 1.185 Å, respectively. The MO of the radical becomes a single occupied molecular orbital (SOMO) and displays nonbonding character with respect to the N–N link (see Fig. 7). The in-plane distortion of the radical geometry determines some bonding character in the N–N link of the SOMO due to overlapping of *p*-orbitals with the same sign on the C(3)–N(7)–N(8) group.

Fig. 7. Single occupied molecular orbital in phenyl diazonium radical.

In the IR-spectrum of the diazenyl radical, the calculated N–N vibration frequency decreases considerably, by 490 cm^{-1}, to 1859 cm^{-1}. This value is higher than the 1400-1600 cm^{-1} of the N=N stretch, but lower than the 2200-2300 cm^{-1} of the N≡N stretch. The N–N bond order decreasing simultaneously with the lengthening of the bond determines a hybrid bond character as suggested by the intermediate value of the vibration frequency. The C–N stretch vibration frequency changes very little, to 1106 cm^{-1}. Also, the spin density is concentrated on the N(7)–N(8) fragment (0.15 and 0.75) respectively.

Consequently, the comparative theoretical analysis of the IR-spectra of aryl diazonium cations and radicals indicates for the diazenyl radical the weakening of the N–N bond with simultaneous small change in the strength of the C–N bond. Therefore, it is conceivable that the nitrogen elimination from the aryl diazonium radical could not be the first step in the Meerwein reaction.

In this context it seems probable the involvement of the triplet excited state of the aryl diazonium cation in the reaction path. The triplet state is found rather unstable in respect to the C–N bond cleavage. It needs an activation energy of only 8.5 kcal/mol as follows from our PM3 CI calculations [40]. The possibility of spin flip during reaction can be provided either by relatively strong spin-orbit coupling (SOC) between π_z and π_y orbitals in the C–N≡N group [41, 42], or by exchange interaction with the $CuCl_2$ catalyst [43].

4. Conclusions

We reported DFT/B3LYP/6-31G** calculations of the electronic structure and vibration IR-spectra of 28 aryl diazonium cations, X-$C_6H_4N_2^+$, with different substituents in the *ortho*-, *meta*- and *para*-

positions. The calculations allowed complete assignment of the absorption bands, the results being in good agreement with available experimental IR frequencies and intensities. The calculated IR spectra may facilitate the future analysis of low frequency vibrations, for which IR spectra are not available at the moment. Moreover, for several absorption bands we established correlations between the vibration frequencies and intensities and the N–N and the C–N bond orders as well as with the nature and force of the mesomeric influence of each substituent. For instance, for the *para*-substituted diazonium cations, when moving from electron donor groups to electron acceptor groups the increase in the N–N bond order is correlated with a strong increase in absorption intensity and a decrease in the frequency.

The calculation of the phenyl diazonium radical with complete geometry optimization indicated a distortion from the linear C–N–N alignment and the lengthening of the C–N and the N–N bonds. The N–N vibration frequency found was 1859 cm^{-1}, 490 cm^{-1} lower than for the cation and intermediate between the N=N stretch and the N≡N stretch. The analysis of the wave function of the unpaired electron carried out for the diazonium radical indicated that the SOMO has a bonding character along the C–N link, hindering nitrogen loss during the Meerwein reaction. Therefore a simple reduction of the diazonium cation can not be the first step in the N_2 elimination. We proposed a tentative involvement of the triplet excited state of the aryl diazonium in the reaction path as a possible alternative. The factors influencing the N_2 elimination from the diazonium cation are still unclear and require further study.

Acknowledgments

We acknowledge financial support from the Ministry of Education and Science of Ukraine and the Ministry of Education and Research of Romania for the bilateral research project (ANCS grant PN2-Capacities-M3 116/2008). Cooperation with Professor Hans Ågren (KTH, Stockholm) is greatly appreciated.

References

1. C. Louault, M. D'Amours, D. Belanger, ChemPhysChem, 9 (2008) 1164.
2. M.G. Paulik, P.A. Brooksby, A.D. Abell, A.J. Downard, J. Phys. Chem. C, 111 (2007) 7808.
3. A. Adenier, E. Cabet-Deliry, A. Chauss, S. Griveau, F. Mercier, J. Pinson, C. Vautrin-Ul, Chem. Mater., 17 (2006) 491.
4. J.L. Bahr, J. Yang, D.V. Kosynkin, M.J. Bronikowski, R.E. Smalley, J.M Tour. J. Am. Chem. Soc., 123 (2001) 6536.
5. J. Pinson, F. Podvorica, Chem. Soc. Rev., 34 (2005) 429.
6. A. J. Downard, Electroanalysis, 12 (2000) 1085.
7. H. Meerwein, E. Büchner, K. van Emster, J. Prakt. Chem., 152 (1939) 237.
8. T. Sandmeyer, Chem. Ber., 17 (1884) 2650.
9. H.H. Hodgson, Chem. Rev., 40 (1947) 251.
10. A.N. Pankratov, O.I. Zhelezko, Int. J. Mol. Sci., 3 (2002) 822.
11. O. Vogl, Ch. S. Rondestvedt (jr), J. Am. Chem. Soc., 77 (1955) 3067.
12. M.D. Obushak, M.B. Lyakhovych, M.I. Ganushchak, Tetrahedron Lett., 39 (1998) 9567.
13. P. Mastrorilli, C.F. Nobile, N. Taccardi, Tetrahedron Lett., 47 (2006) 4759.
14. L.A. Kazitsyna, S.V. Pasynkevich, and O.A. Reutov, Dokl. AN SSSR, 141 (1961) 624.
15. L.A. Kazitsyna, O.A. Reutov, and Z.F. Buchkovskii, Zh. Obshch. Khim., 30 (1960) 1008.
16. L.A. Kazitsyna, O.A. Reutov, B.S. Kikot', Zh. Obshch. Khim., 33 (1963) 1561.
17. Y.N. Panchenko, J. Struct. Chem., 40 (1999) 451.
18. H. Yoshida, A. Ehara, H. Matsuura, Chem. Phys. Lett., 325 (2000) 477.
19. E.R. Davidson, Int. J. Quantum Chem., 69 (1998) 241.

20. E.P. Koval'chuk, N.I. Ganushchak, I.N. Krupak, N.D. Obushak, and O.P. Polishchuk, Zh. Obshch. Khim., 58 (1988) 2370.
21. V.M. Traiger, I.L. Bagal, Zh. Org. Khim., 10 (1974) 2494.
22. I.L. Bagal, N.D. Stepanov, A.V. El'zov, Zh. Org. Khim., 18 (1982) 18.
23. S.J. Weiner, P.A. Kollman, D.T. Nguyen, D.A. Case, J. Comp. Chem., 7 (1986) 230.
24. J.J.P. Stewart, J. Comp. Chem., 10 (1989) 221.
25. W. Kohn, L.J. Sham, Phys. Rev. A, 140 (1965) 1133.
26. A.D. Becke, J. Chem. Phys. 98 (1993) 5648;
27. C. Lee, W. Yang, R.G. Parr, Phys. Rev. B, 37 (1988) 785.
28. W.J. Hehre, L. Radom, P. v. R. Schleyer, J.A. Pople, Ab Initio Molecular Orbital Theory; Wiley, New York, 1986.
29. H.B. Schlegel, J. Comp. Chem., 3 (1982) 214.
30. B. Minaev , S. Bondarchuk , A. Minaev. Proceedings of the Nano-Sol-Net Int. Symposium "Trends in organic electronics and hybrid photovoltaics". Constanța, 2006. P. 54.
31. M.J. Frisch et al., Gaussian 03, Revision B.03, Gaussian Inc., Pittsburgh, PA, 2003.
32. Chr. Römming, Acta Chem. Scand., 17 (1963) 1444.
33. M. Cygler, M. Przybylska, R. Elofson, Can. J. Chem., 60 (1982) 2852.
34. L.A. Kazitsyna, B.S. Kikot', L.D. Ashkinadze, and O. A. Reutov, Dokl. AN SSSR, 151 (1963) 573.
35. A.P. Scott, L. Radom *J. Phys. Chem.* 100 (1996) 16502.
36. J.P. Merrick, D. Moran, L. Radom *J. Phys. Chem. A*, 111 (2007) 11683.
37. A.E. Agronomov. Collected Chapters of Organic Chemistry. Khimiya: Moscow, 1990.
38. E.F. Healy, A. Holder, J. Mol. Struct. (Theochem), 281 (1993) 141.
39. M.D. Newton, J. Chem. Phys., 48 (1968) 2825.
40. B.F. Minaev, S.V. Bondarchuk, Russ. J. Appl. Chem. (in press).
41. B.F. Minaev, H. Ågren, J. Mol. Struct. (Theochem), 434 (1998)193.
42. B.F. Minaev, H. Ågren, J. Mol. Struct. (Theochem), 492 (1999) 53.
43. B.F. Minaev, J. Mol. Catalysis A: Chem., 171 (2001) 53.